Gap solitons in parity–time complex superlattice with dual periods*

Wang Hong-Cheng(王红成)[a)†], Ling Dong-Xiong(凌东雄)[a)], Zhang Shao-Qiang(张绍强)[a)], Zhu Xing(朱 兴)[b)], and He Ying-Ji(何影记)[c)]

[a)] College of Electronic Engineering, Dongguan University of Technology, Dongguan 523808, China
[b)] State Key Laboratory of Optoelectronic Materials and Technologies, Sun Yat-Sen University, Guangzhou 510275, China
[c)] School of Electronics and Information, Guangdong Polytechnic Normal University, Guangzhou 510665, China

(Received 11 October 2013; revised manuscript received 7 November 2013; published online 10 April 2014)

A theory is presented to investigate the existence and propagation stability of gap solitons in a parity–time (PT) complex superlattice with dual periods. In this superlattice, the real and imaginary parts are both in the form of superlattices with dual periods. In the self-focusing nonlinearity, PT solitons can exist in the semi-infinite gap. However, only those gap solitons with low powers can propagate stably, whereas the high-power solitons present periodic oscillation and simultaneously suffer energy decay. In the self-defocusing nonlinearity, PT solitons only exist in the first gap and all these solitons are stable.

Keywords: spatial soliton, parity–time soliton, gap soliton, superlattice

PACS: 42.65.Tg, 42.65.Jx, 42.65.Wi **DOI:** 10.1088/1674-1056/23/6/064208

1. Introduction

Since the first introduction of parity–time (PT) optics in 2005,[1] a great deal of research interest has been aroused in the light propagation in PT-symmetric potentials. A PT-symmetric optical potential has been realized by the careful distribution of gain and loss so that it satisfies the PT symmetry $V(x) = V^*(-x)$, where x is the spatial coordinate and "$*$" denotes complex conjugation. That is, the refractive index profile is even and the gain-loss profile is odd. Such optical PT media have been created experimentally[2] and the optical systems which have PT-symmetric potentials have been formulated.[3] Very recently, in the context of nonlinear optics, the propagation of optical beams in PT nonlinear optical lattices was investigated and gap solitons were found to exist stably.[4] The existence, stability, and propagation dynamics of the one-dimensional (1D) and two-dimensional (2D) optical solitons in a PT-symmetric nonlinear lattice[5] and linear lattice[6,7] have been examined in detail. By using PT-symmetric potentials, gray solitons[8] and vector solitons[9] have also been obtained and investigated. In PT-symmetric mixed linear-nonlinear optical lattices, propagation dynamics of fundamental and dipole solitons have also been investigated.[10,11] Very recently, the stability properties of optical solitons were investigated in a chirped PT-symmetric lattice whose frequency changes in the transverse direction.[12]

On the other hand, optical superlattices have some fascinating properties because the structures exhibit collective properties not shared by either constituent and these properties can be controlled through the variation of the structural parameters.[13] Thus far, considerable attention has been paid to the soliton phenomena in superlattices with PT-symmetric potential.[14–17] In these studies, the real part of the lattice potential is constituted by two periodical lattices with different periods, while the imaginary part is in the simple form of a periodic lattice. It has been found that gap solitons can stably exist in the PT periodic lattices whose real parts are superlattices. However, there are no reports on the existence stability of bright spatial solitons with a complete PT complex superlattice. In this potential, the real and imaginary parts are both in the form of superlattices. In other words, both the real and imaginary parts of the potential are composed of two periodical potentials with different periods. In general, a complex superlattice that simultaneously exhibits a symmetric refractive index distribution and an antisymmetric gain/loss profile can be readily built by judiciously incorporating, in a balanced way, regions having optical gain and loss.[2] So, the imaginary part of the lattice can also have the superlattice potential, and it has the same period as the real part. In this paper, we investigate the existence and stability of gap solitons in the PT-symmetric superlattice which has dual periods in both the real and imaginary parts. Some novel soliton properties are revealed in this new system.

2. Theoretical model

Beam propagation in the PT complex superlattice with Kerr nonlinearity obeys the following normalized 1D

*Project supported by the National Natural Science Foundation of China (Grant No. 61308019) and the Foundation for Distinguished Young Talents in Higher Education of Guangdong Province, China (Grant No. Yq2013157).

†Corresponding author. E-mail: hc_wang@126.com

© 2014 Chinese Physical Society and IOP Publishing Ltd

Schrödinger equation:

$$\mathrm{i}\frac{\partial u}{\partial z}+\frac{\partial^2 u}{\partial x^2}+V_0\left[v(x)+\mathrm{i}w_0 w(x)\right]u+\sigma|u|^2 u=0, \quad (1)$$

where u is the complex field amplitude, $\sigma=\pm1$ denotes the focusing and defocusing nonlinearity, x and z are the dimensionless transverse and longitudinal coordinates, respectively, $v(x)$ and $w(x)$ are the real part and image parts of the complex potential, respectively, V_0 denotes the lattice depth, and w_0 is a parameter controlling the relative depth of the imaginary part. In the context of a superlattice with complete PT-symmetric potential, both the real and imaginary parts of the potential are in the superlattice form with dual periods. Therefore, we have $v(x)=\varepsilon_1\cos^2 x+(1-\varepsilon_1)\sin^2(2x)$, and $w(x)=\varepsilon_2\sin(2x)+(1-\varepsilon_2)\sin(4x)$, where ε_1 and ε_2 are the parameters controlling the relative strength of the superlattice, and their values are both limited to a range between 0 and 1. Typical profiles of the superlattice when $\varepsilon_1=0.6$, $\varepsilon_2=0.4$, and $V_0=6$ are shown in Fig. 1(a). In Fig. 1(a), one can see that both the real and imaginary parts of the PT superlattice are composed of two periodical lattices. The real and imaginary parts have the same periods. Obviously, the periodic refractive-index modulation obeys the PT-symmetry.

We search for the stationary solutions of Eq. (1) in the form of $u(x)=f(x)\exp(\mathrm{i}\mu z)$, where $f(x)$ is a complex function, and μ is the corresponding real propagation constant. By substituting this form into Eq. (1), we have the function $f(x)$ that should satisfy the following equation:

$$-\mu f+\frac{\partial^2 f}{\partial x^2}+V_0\left[v(x)+\mathrm{i}w_0 w(x)\right]f+\sigma|f|^2 f=0. \quad (2)$$

In order to understand the origin of gap solitons in complex superlattice, we first investigate their bandgap structure of superlattice of this kind. Obviously, the linear version of Eq. (2) is

$$-\mu f+\frac{\partial^2 f}{\partial x^2}+V_0\left[v(x)+\mathrm{i}w_0 w(x)\right]f=0. \quad (3)$$

From the Bloch theorem, the eigenfunction of Eq. (3) is in the form of $f=F_k\exp(\mathrm{i}kx)$, where k is the Bloch wave number in the irreducible Brillouin zone ($-1\le k\le 1$), and F_k is a periodic function of x with the same period as the real part $v(x)$ and the imaginary part $w(x)$ of the superlattices. Substituting the Bloch solution into Eq. (3), we can obtain the eigenvalue equation

$$\left(\frac{\partial^2}{\partial x^2}+2\mathrm{i}k\frac{\partial}{\partial x}-k^2\right)F_k+V_0\left[v(x)+\mathrm{i}w_0 w(x)\right]F_k=\mu F_k. \quad (4)$$

Obviously, the values of μ and k are related to each other by the relation $\mu=\mu(k)$, which is called the diffraction relation, and all admissible values of μ form the continuous spectrum of Eq. (3). Using the plane wave expansion method to solve Eq. (4) numerically, we can obtain the band structure. Different values of the strength parameters lead to different band structures. In the case similar to a simple PT lattice, there is a PT threshold w_0^{th} in the PT superlattice, below which all the propagation eigenvalues for every band and every Bloch wave number k are real. Above this threshold, an abrupt phase transition occurs because of spontaneous symmetry breaking and as a result the spectrum is partially complex. For example, we take $\varepsilon_1=0.6$, $\varepsilon_2=0.4$, and $V_0=6$, the diffraction relations are shown in Figs. 1(b)–1(e). In the numerical calculations, we can find $w_0^{\mathrm{th}}=0.385$. Below this transition point, all the

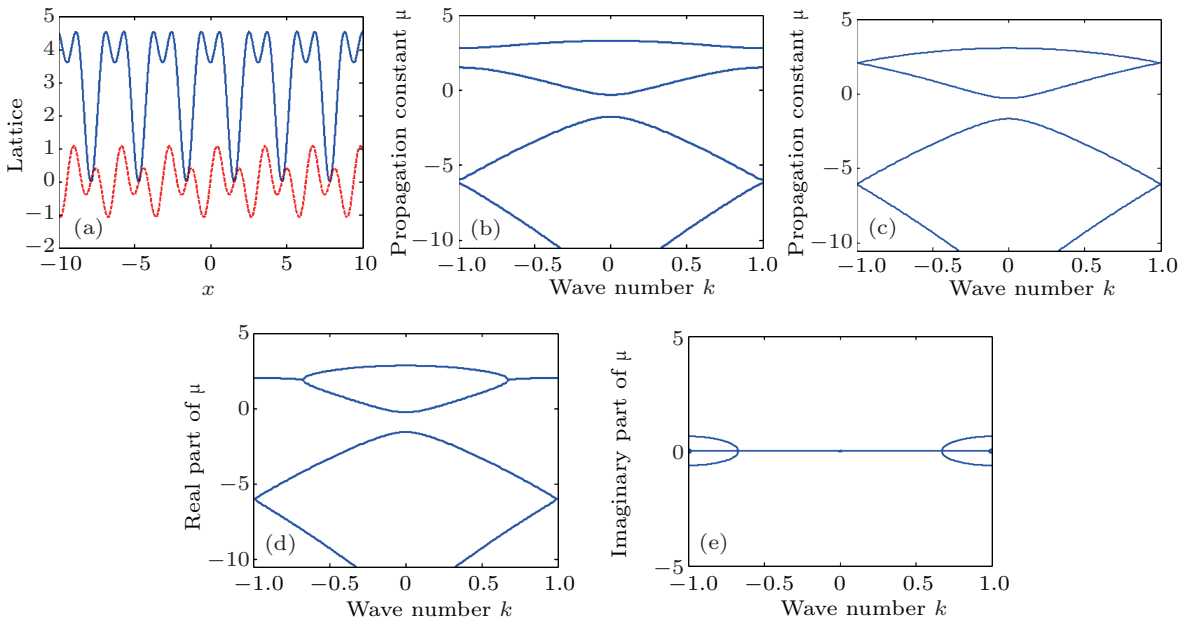


Fig. 1. (color online) (a) Typical profiles of PT superlattice (solid: real part; dashed: imaginary part). (b)–(e) Diffraction relations of PT lattices for three w_0 values of (b) 0.2, (c) 0.385, and (d) and (e) 0.5 at $\varepsilon_1=0.6$, $\varepsilon_2=0.4$, and $V_0=6$.

eigenvalues are real, and all the forbidden gaps are open. Figure 1(b) gives the band structure when $w_0 = 0.2$. As shown in Fig. 1(b), the semi-infinite gap is $\mu \geq 3.2754$, and the first gap is $1.4972 \leq \mu \leq 2.79$. However, at the transition point $w_0^{\text{th}} = 0.385$, some band gaps at the edges of the Brillion zone are close to each other, which can be easily seen from Fig. 1(c). When w_0 exceeds this critical vale, complex eigenvalues μ bifurcate out simultaneously, and the first and second band start to merge together to form oval-like structures. Figures 1(d) and 1(e) show the real and imaginary parts of the band structure when $w_0 = 0.5$, respectively. From these figures, one can see that the imaginary eigenvalue bifurcates from the band edge, which corresponds to $k = \pm 1$.

3. Gap solitons and their stabilities

The lattice soliton solutions of Eq. (2) exist when μ lies inside the band gaps of the linear system for w_0 below and above the phase transition point. Above the phase transition point, the PT symmetry is broken. In this case, soliton solutions can also be found, but these solitons are unstable and decay quickly. This is because linear waves are amplified exponentially during propagation, thus any solitons would also be unstable to perturbations. So we just consider those values of w_0 below w_0^{th}. To demonstrate the existence and stability of gap soliton better, we set $w_0 = 0.2$ as an example hereafter. Due to the existence of the imaginary part of the lattice potential, the soliton solution also has an imaginary part. So, substituting $f(x) = h(x) + \mathrm{i}e(x)$ into Eq. (2), we obtain the two coupled equations:

$$h_{xx} + V_0 (vh - w_0 we) + \sigma \left(e^2 h + h^3\right) = \mu h, \tag{5a}$$

$$e_{xx} + V_0 (ve - w_0 wh) + \sigma \left(h^2 e + e^3\right) = \mu e, \tag{5b}$$

where h and e are the real functions. Numerically solving Eqs. (5a) and (5b) by a modified squared-operator method,[18] we can obtain real part $h(x)$ and imaginary part $e(x)$. To analyze the linear stabilities of these solutions in the PT complex periodic superlattice, we add perturbations $g(x)$ and $t(x)$ to the solution $f(x)$, i.e.,

$$\begin{aligned} u(x,z) \;=\; & \exp(\mathrm{i}\mu z)\{f(x) + [g(x) - t(x)]\exp(\delta z) \\ & + [g(x) + t(x)]^* \exp(\delta^* z)\}, \end{aligned} \tag{6}$$

where both $g(x)$ and $t(x)$ are far smaller than $f(x)$, and δ is the complex growth rate. By substituting Eq. (6) into Eq. (1) and linearizing the resulting equation, we have the following coupled equations:

$$\begin{aligned} \mathrm{i}\delta g \;=\; & \frac{\partial^2 t}{\partial x^2} - \mu t + V_0 (vt - \mathrm{i}w_0 wg) \\ & + \sigma \left[2|f|^2 t - \frac{1}{2}\left(f^2 - f^{*2}\right) g - \frac{1}{2}\left(f^2 + f^{*2}\right) t\right], \end{aligned} \tag{7a}$$

$$\begin{aligned} \mathrm{i}\delta t \;=\; & \frac{\partial^2 g}{\partial x^2} - \mu g + V_0 (vg - \mathrm{i}w_0 wt) \\ & + \sigma \left[2|f|^2 g + \frac{1}{2}\left(f^2 - f^{*2}\right) g + \frac{1}{2}\left(f^2 + f^{*2}\right) t\right]. \end{aligned} \tag{7b}$$

Equations (7a) and (7b) can also be solved numerically by the Newton-conjugate gradient method.[19] If $\mathrm{Re}(\delta) > 0$, the small perturbation will undergo an exponential growth, and the solitons are linearly unstable. Otherwise, they are linearly stable.

3.1. Superlattice solitons in self-focusing nonlinearity

In this section, we let $\sigma = +1$ and consider the existence and stability of PT solitons in self-focusing nonlinearity. Let the power of a soliton be defined as $P(\mu) = \int_{-\infty}^{\infty} |f(x;\mu)|^2 \mathrm{d}x$, their power curves of fundamental solitons are displayed in Fig. 2(a). According to the numerical calculations, we can deduce that the solitons can exist in the semi-infinite bandgap. However, no solitons can be found in the first gap. In the semi-infinite gap, one can see that the soliton power increases with the value of the propagation constant increasing. The solitons near the first Bloch band have lower powers, and those far from the first band have higher powers. Through the analyses of linear stability spectra, the PT solitons in the semi-infinite gap are stable only in a finite interval. Obviously, the solitons are stable only when $3.2754 < \mu < 6.98$ (solid curve), whereas those solitons whose propagation constants are above 6.98 are unstable (dashed curve). This result can also be concluded from Fig. 2(b), which shows the relation between the instability growth rate $\mathrm{Re}(\delta)$ and the propagation constant. In this inset, the instability growth rate $\mathrm{Re}(\delta)$ is always zero when $3.2754 < \mu < 6.98$. Therefore, the solitons are stable in this parameter region. When $\mu > 6.98$, $\mathrm{Re}(\delta)$ has non-zeroed values, the solitons are unstable. To give some typical examples, we solve Eq. (5) numerically and plot the profiles of PT solitons at $\mu = 3.3$, $\mu = 4.0$, $\mu = 9.5$, and $\mu = 11.0$ in Figs. 2(c), 2(d), 2(e), and 2(f), respectively. These solitons, bifurcating out of the upper edge of the first Bloch band, are composed of real and imaginary parts, due to the complexity of the lattice. The real profiles (dashed) are even symmetric while the imaginary profiles (solid) exhibit as odd symmetric. As seen from Fig. 2(c), gap solitons near the band edge are very similar to low-amplitude wave packets when $\mu = 3.3$. As the propagation constant μ increases, those side humps disappear gradually and the energy accumulates towards the central hump. When μ increases to a medium value (e.g., 4.0), the real part of this PT soliton has only one hump [see Fig. 2(d)]. If μ is set to be a large value, the soliton presents a simple single-hump profile [see Figs. 2(e) and 2(f)]. Comparing these figures with each other, one can find that the soliton width decreases as the value of μ increases.

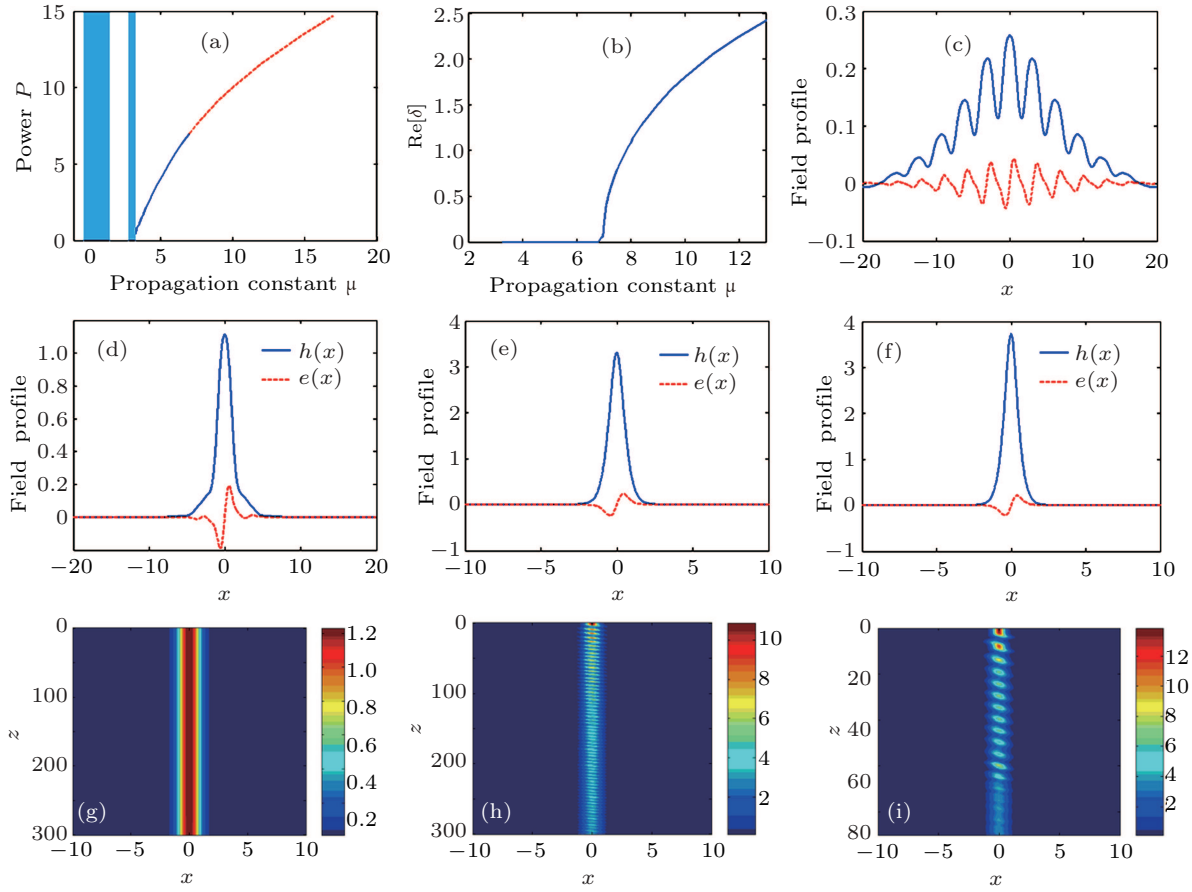


Fig. 2. (color online) Gap solitons and their propagation stabilities in the semi-infinite gap under focusing nonlinearity ($\sigma = +1$): (a) power versus propagation constant μ; (b) instability growth rate versus propagation constant μ; (c)–(f) field profiles (blue: real part; red: imaginary part) of gap solitons at $\mu = 3.3$, 4.0, 9.5, and 11; (g)–(i) corresponding propagations of gap solitons shown in panels (d), (e), and (f) under the perturbation of a 10% random noise.

To validate the stability properties, we add a random noise (10% of the soliton amplitude) to the soliton solution and perform direct numerical simulations of Eq. (1). Figures 2(g), 2(h), and 2(i) show the propagation behaviors of PT superlattice solitons at $\mu = 4.0$, 9.5, and 11.0, respectively. As shown in Fig. 2(g), the solitons at low μ values can propagate stably and keep their shapes under the perturbation of 10% white noise. If we increase the value of μ, the propagation becomes unstable. As a consequence of the competition between the nonlinearity and the potential of the PT lattice, the peak amplitude experiences a damping oscillation when $\mu = 9.5$ [shown in Fig. 2(h)]. After about 300 dimensionless propagation lengths, the gap soliton cannot survive and nearly disappears in the background. For a large μ [e.g., $\mu = 11$ shown in Fig. 2(i)], the gap soliton decays more quickly and nearly disappears in the background after 80 dimensionless propagation lengths.

3.2. Superlattice solitons in self-defocusing nonlinearity

Next we consider PT solitons in the self-defocusing nonlinearity, and the nonlinearity coefficient σ is chosen to be -1. Again, for $w_0 = 0.2$, the profiles of PT solitons at $\mu = 1.6$, 2.0, 2.75 are obtained in Figs. 3(b), 3(c), and 3(d), respectively. Their power curve is displayed in Fig. 3(a) with stability results indicated. Figure 3(a) indicates that the solitons only exist in the first gap under self-defocusing nonlinearity. Near the lower edge of the first band, the real parts of the solitons are similar to large amplitude Bloch waves [see Fig. 3(b)], while near the upper edge of the second gap, they are similar to low amplitude Bloch waves [see Fig. 3(d)]. In other words, the solitons can bifurcate from both the lower edge of the first and upper edge of the second Bloch band. When $1.4972 \leq \mu \leq 2.79$, the instability growth rate δ is always zero, and therefore all these solitons are linearly stable. To confirm this result, we carry out direct numerical simulations after having added 10% white noise to the solitons. Figures 3(e), 3(f), and 3(g) show the stable propagation of the solitons whose optical filed profiles are shown in Figs. 3(b), 3(c), and 3(d), respectively. It is found that all these solitons are strong enough to overcome the perturbation of a 10% random noise and remain robust in the PT superlattice even after 300 units of dimensionless propagation lengths.

3.3. Influence of superlattice on PT solitons

As described in Section 2, the relative lattice depth of the imaginary part and the profile of the superlattice can affect the PT symmetry. If the value of w_0 is above the critical

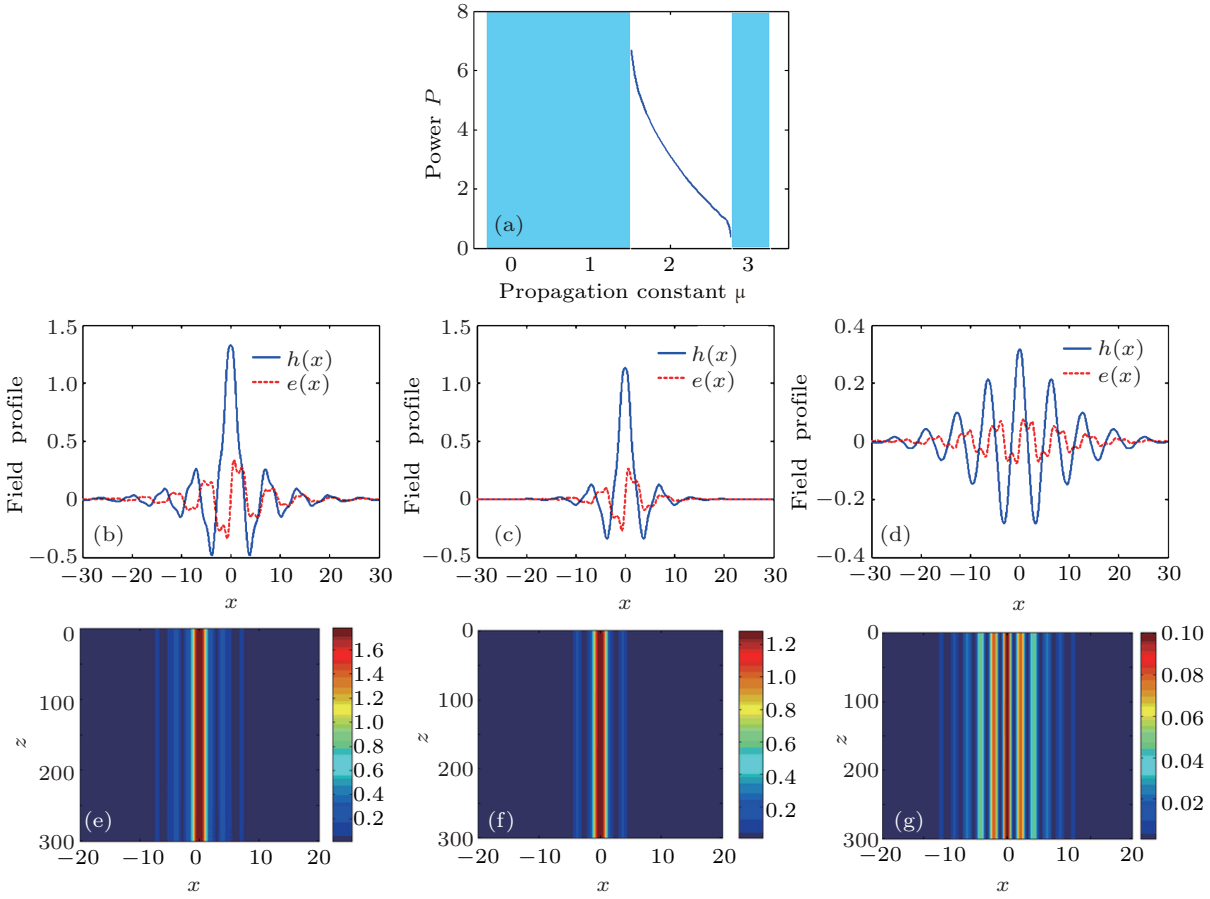


Fig. 3. (color online) Gap solitons and their propagation stabilities in the first gap under self-defocusing nonlinearity: (a) power versus propagation constant μ; (b)–(d) profiles of gap solitons at $\mu = 1.6, 2.0, 2.75$ (blue: real part; red: imaginary part); (e)–(g) stable propagations of gap solitons shown in panels (b), (c), and (d) under the perturbation of 10% random noise, respectively.

value 0.385, the PT symmetry is broken when $\varepsilon_1 = 0.6$, $\varepsilon_2 = 0.4$, and $V_0 = 6$. When the PT symmetry remains unchanged, w_0 affects the amplitude of the imaginary part of the soliton. The larger the value of w_0, the larger the imaginary part is. The PT symmetry can also be affected by the parameters ε_1 and ε_2. If we choose $\varepsilon_1 = 0.3$ or $\varepsilon_2 = 0.7$ while other parameters remain the same as those in Fig. 1(a), the eigenvalue spectrum is partially complex and the PT-symmetry is broken. On the other hand, the parameter ε_1 can affect the soliton profiles. Figure 4(a) shows the soliton profile when $\mu = 4.0$ and $\sigma = +1$ while figure 4(b) shows the soliton profile when $\mu = 2.2$ and $\sigma = -1$. The values of the other parameters are $\varepsilon_1 = 0.3$, $\varepsilon_2 = 0.4$, $w_0 = 0.1$, and $V_0 = 6$. From these figures, we can see that the real part of the soliton profile is concave in the center whatever type the nonlinearity is. This concavity always appears when $\varepsilon_1 < 0.5$ because of the influence of the real part of the superlattice potential.

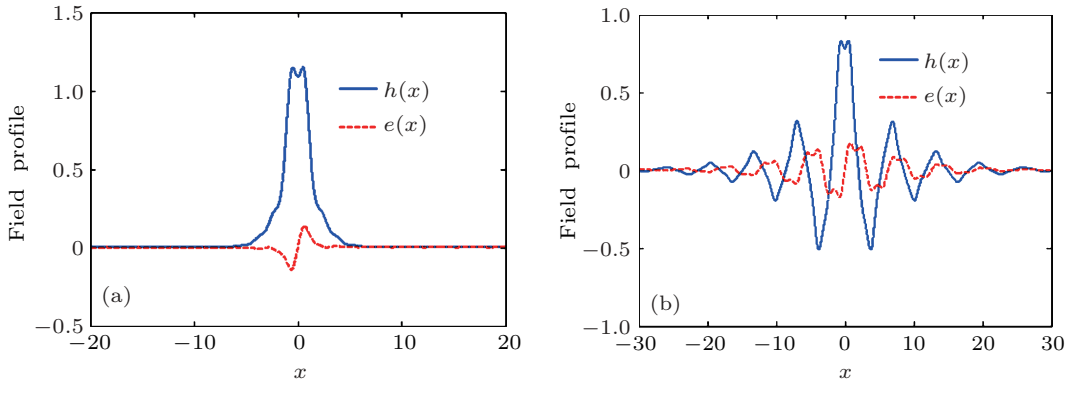


Fig. 4. (color online) Soliton profiles when $\varepsilon_1 = 0.3$, $\varepsilon_2 = 0.4$, $w_0 = 0.1$, and $V_0 = 6$: (a) $\mu = 4.0$, $\sigma = +1$; (b) $\mu = 2.2$, $\sigma = -1$.

4. Conclusions

In this paper, we investigate the existence and stability properties of fundamental gap solitons in PT-symmetric complex superlattices with dual periods in both the real and imaginary parts. It is found that PT solitons can exist in the semi-infinite gap under self-focusing nonlinearity and in the first gap under self-focusing nonlinearity. In the self-focusing nonlinearity, those solitons with low powers are stable but those with high powers propagate with periodic oscillations and simultaneously their energies decay during the propagation. In the defocusing nonlinearity, the PT soliton in the whole first gap can propagate stably even under the perturbation of 10% white noise.

References

[1] Ruschhaupt A, Delgado F and Muga J G 2005 *J. Phys. A: Math. Gen.* **38** L171

[2] Rüter C E, Makris K G, El-Ganainy R, Christodoulides D N, Segev M and Kip D 2010 *Nat. Phys.* **6** 192

[3] El-Ganainy R, Makris K G, Christodoulides D N and Musslimani Z H 2007 *Opt. Lett.* **32** 2632

[4] Musslimani Z H, Makris K G, El-Ganainy R and Christodoulides D N 2008 *Phys. Rev. Lett.* **100** 030402

[5] Abdullaev F Kh, Kartashov Y V, Konotop V V and Zezyulin D A 2011 *Phys. Rev. A* **83** 041805

[6] Shi Z, Jiang X, Zhu X and Li H 2011 *Phys. Rev. A* **84** 053855

[7] Nixon S, Ge L and Yang J 2012 *Phys. Rev. A* **85** 023822

[8] Li H, Shi Z, Jiang X and Zhu X 2011 *Opt. Lett.* **36** 3290

[9] Kartashov Y V 2013 *Opt. Lett.* **38** 2600

[10] He Y, Zhu X, Mihalache D, Liu J and Chen Z 2012 *Phys. Rev. A* **85** 013831

[11] Huang C, Li C and Dong L 2013 *Opt. Express* **21** 3917

[12] Li C Y, Huang C M and Dong L W 2013 *Chin. Phys. B* **22** 074209

[13] Chen W and Mill D L 1987 *Phys. Rev. Lett.* **58** 160

[14] Driben R and Malomed B A 2011 *Opt. Lett.* **36** 4323

[15] Alexeeva N V, Barashenkov I V, Sukhorukov A A and Kivshar Y S 2012 *Phys. Rev. A* **85** 063837

[16] Zhu X, Wang H, Zheng L X, Li H and He Y J 2011 *Opt. Lett.* **36** 2680

[17] Hu S M and Hu W 2012 *Chin. Phys. B* **21** 024212

[18] Yang J and Lakoba T I 2007 *Stud. Appl. Math.* **118** 153

[19] Yang J 2010 *Nonlinear Waves in Integrable and Nonintegrable Systems* (Philadelphia: SIAM)